Electronic Supplementary Information

Sensitive Photoelectrochemical Methyltransferase Activity Assay Based on A Novel "Z-scheme" CdSe QDs/afGQDs Heterojunction and Multiple Signal Amplification Strategies

Leixia Meng, Ke Xiao, Yanmei Li, Xiaohua Zhang, Cuicui Du, Jinhua Chen*

State Key Laboratory of Chemo/Biosensing and Chemometrics, College of Chemistry and Chemical Engineering, Hunan University, Changsha, 410082, People's Republic of China

List of Contents:

* Corresponding author. Tel.: +86-731-88821848

E-mail address: chenjinhua@hnu.edu.cn

1. Materials and apparatus

Cadmium chloride hemipentahydrate ($CdCl_2 \cdot 2.5H_2O$), sodiumborohydride ($NaBH_4$), glutaraldehyde (GLD, 25 wt.% aqueous solution), manganese sulfate monohydrate ($MnSO_4 \cdot H_2O$), potassium permanganate ($KMnO_4$), ammonia solution, tris-(hydroxymethyl)aminomethane (Tris) and ascorbic acid (AA) were obtained from Sinopharm Chemical Reagent Co., Ltd. (Beijing, China). Graphene oxide solution (GO, 5 mg mL^{-1}) prepared by Hummers method was purchased from NewMater New Nanotechnology Co., Ltd. (Guangyuan, China). Hydrazinium hydrate ($H_4N_2 \cdot H_2O$, 80 wt.%) were purchased from Shanpu Chemical Co., Ltd. (Shanghai, China). Hydrogen tetrachloroaurate (III) trihydrate ($HAuCl_4 \cdot 3H_2O$, 99.999%), poly(diallyldimethylammonium chloride) (PDDA) (MW= 200,000-350,000, 20% (m:m), in water), PAMAM dendrimer (ethylenediamine core, generation 5.0 solution, 5 wt% in methanol), 5-Azacytidine (5-Aza) and 5-aza-2′-deoxycytidine (5-Aza-dC) were purchased from Sigma-Aldrich Co., Ltd. (USA). Selenium metal powder (Se), mercaptopropionic acid (MPA, 98%), 1-ethyl-3-(3-dimethylaminopropyl) carbodiimide hydrochloride (EDC) and 4-chloro-1-naphthol (4-CN) were obtained from Macklin Reagent Co., Ltd. (Shanghai, China). N-hydroxysuccinimide (NHS) were obtained from Yuanye Biotechnology Co., Ltd. (Shanghai, China). Bovine serum albumin (BSA) and tris (2-carboxyethyl) phosphinehydrochloride (TCEP) were supplied from Sangon Biotechnology Co., Ltd. (Shanghai, China). CpG methyltransferase (M.SssI MTase), sadenosyl-L-methiolnine (SAM), restriction endonuclease HpaII, HaeIII methyltransferase (HaeIII MTase), AluI methyltransferase (AluI MTase), 10 × NEBuffer 2, 10 × CutSmart buffer were

purchased from New England BioLabs (Ipswich, MA, USA). All the synthetic oligonucleotides were supplied from Sangon Biotechnology Co., Ltd. (Shanghai, China) and the sequences of those are shown in Table S1. The indium tin oxide (ITO) glass was obtained from Zhuhai Kaivo Electronic Components Co., Ltd. (China). All the reagents were analytical grade and used without further purification. Ultrapure water (18.2 MΩ cm^{-1}) obtained from a Millipore system (Millipore Corp., Bedford, MA) was used throughout.

Table S1. The DNA sequences used in this work.

Name	Sequence (5′→3′)
DNA1	NH_2-$(CH_2)_6$-GCT CCG GAT CTC CCT TCC CAG GAC GC
DNA2	SH-$(CH_2)_6$-GCG TCC TGG GAA GGG AGA TCC GGA GC

[a] The specific recognition sequences for both M.SssI MTase and HpaII in DNA 1 and DNA2 are marked in red.

The UV absorption spectra were obtained from a UV-2100 spectrophotometer (Beijing Lab Tech, China). Fluorescence spectrum was recorded on an F-4600 spectrophotometer (Hitachi, Japan). The morphology and structure of the prepared samples were characterized by scanning electron microscopy (SEM, JSM-6700F, Japan) and transmission electron microscopy (TEM, Tecnai G2 F20 S-TWIN, Holland). A PLS-SXE 300 Xe lamp fitted with a 420 nm UV filter was used as the light source to produce visible light in the PEC test. The electrochemical and

photoelectrochemical measurements were performed on an electrochemical workstation (CHI 660D, Chenhua Instrumental Co., Shanghai, China) with a typical three-electrode configuration at ambient temperature. The modified ITO slice with a geometrical area of 0.25 cm^2 was utilized as the working electrode. A Pt wire with a diameter of 1 mm was used as auxiliary electrode, and reference electrode was a saturated calomel electrode (SCE). 0.1 M phosphate buffer solution (PBS, pH 7.4) containing 0.1 M AA was utilized as the photoelectrochemical electrolyte solution.

2. Preparation of P-rGO

Poly (diallyl dimethylammonium chloride) (PDDA)-modified reduced graphene oxide (P-rGO) was prepared via the in-situ reduction of GO in the presence of PDDA as reported literature with slight modification.[1] In brief, 10 mL of 5 mg mL^{-1} GO solution was mixed with 90 mL ultrapure water and sonicated for 30 min. Then, 0.5 mL of 20% PDDA was added to the mixture under stirring for another 30 min. After that, 0.5 mL of 80 wt.% hydrazine hydrate was added and the solution was stirred for 24 h at 90 ° C. Finally, the P-rGO was obtained by filtration, washed with ultrapure water, and then re-dispersed in ultrapure water for future use.

3. Preparation of CdSe QDs

CdSe quantum dots (QDs) was prepared according to the previous report with minor modification.[2] In brief, NaHSe was obtained via adding 7.6 mg $NaBH_4$ into 5mL ultrapure water under nitrogen stream, then adding 7.9 mg Se powder.

Meanwhile, 45.7 mg $CdCl_2 \cdot 2.5H_2O$ and 44 μL MPA were dissolved in 50 mL ultrapure water and stirred at 100 °C with nitrogen bubbling. Under nitrogen atmosphere, the pH was adjusted to 11 through dropping1 M NaOH, and the newly prepared NaHSe was quickly injected into this mixture. The reaction was kept for 4 h to form a clear orange solution of MPA-CdSe QDs. Finally, CdSe QDs was obtained by centrifugation and washed with ethanol. For future use, 1 mg mL^{-1} CdSe QDs solution was prepared and stored in the dark at 4 °C.

4. Preparation of afGQDs

The GQDs were prepared by the reported method.[3] The amino functionalization of GQDs (afGQDs) was carried out through a hydrothermal route. Typically, the prepared GQDs aqueous solution (6 mL) was mixed with 6 mL of 28 wt% ammonia solution in a 50 mL round bottom flask. After stirring for 1 h, the mixture was transferred to a 20 mL Teflon-lined autoclave and heated at 200 °C for 10 h. After cooling to room temperature, the light yellow supernatant (the desired afGQDs) was heated to 100 °C for 1 h to vaporize excess ammonia, and the solution was further dialyzed in a dialysis bag (retained molecular weight: 1000 Da). The purified afGQDs were kept in ultrapure water and stored in the dark at 4 °C for later use.

5. Preparation of DNA2-Au-PAMAM-Mn^{2+} bioconjugation

The DNA2-Au-PAMAM was prepared according to the literature with minor modification.[4] At first, the Au-PAMAM dendrimer (Au-PAMAM) was prepared as

follows: 1.333 mL ultrapure water was added to 1.667 mL of 5.0 wt% PAMAM dendrimer solution, and then 2 mL of 24.28 mM $HAuCl_4$ was added. To make $AuCl_4^-$ attach to the amino groups of the PAMAM dendrimer, the mixture was stirred energetically for 1 h at room temperature. Subsequently, 2 mL of 0.5 M freshly prepared ice-cold $NaBH_4$ solution was quickly added to the above solution under stirring. When the color of the solution was changed from light yellow to red-brown, the Au-PAMAM was formed. After centrifugation at 15000 rpm for 30 min, the sediment was resuspended in 1mL ultrapure water and stored at 4 °C.

Before use, DNA2 was dissolved in 10 mM Tris-HCl buffer solution (0.1 M NaCl, 10 mM TCEP, pH 7.4) and incubated for 1 h in a black medium to decrease disulfide bonds. Then, 500 μL of 10 mM Tris-HCl (0.1 M NaCl , pH 7.4) was added into 500 μL of the above-prepared AuNP-PAMAM solution, and then 50 μL of 2 μM DNA2 was injected into the above solution. Subsequently, the mixture was gently shaken for 16 h at 4 °C. After centrifugation at 15000 rpm, DNA2-Au-PAMAM was obtained and resuspended into 1 mL of 10 mM Tris-HCl (0.1 M NaCl , pH 7.4) and stored at 4 °C.

The DNA2-Au-PAMAM-Mn^{2+} was synthesized based on the good adsorption property of the amino groups on the PAMAM dendrimer to the metal ion. The mixture containing 1 mL of the above prepared DNA2-Au-PAMAM and 500 μL of 0.1 M $MnSO_4$ solution was shaken for 12 h at 4 °C. After centrifugation at 15000 rpm, the DNA2-Au-PAMAM-Mn^{2+} was obtained and re-dispersed in 1 mL of 10 mM Tris-HCl (0.1 M NaCl , 20 mM $MgCl_2$, pH 7.4) containing 1.0 % BSA and stored at 4 °C

for future use.

6. Construction of the "Z-scheme" PEC biosensor and methyltransferase activity assay.

Before modification, ITO electrodes were sonicated successively in acetone, ethanol/1 M NaOH (1:1, *v*/*v*) and ultrapure water. After dried at 60 °C, P-rGO solution (20 μL, 0.2 mg mL^{-1}) was dripped on the surface of ITO electrode to firmly immobilize CdSe QDs via electrostatic interaction between the positive-charged P-rGO and negative-charged CdSe QDs. After dried in air, the ITO/P-rGO electrode was coated with 20 μL of 1.5 mg mL^{-1} CdSe QDs. Then, The ITO/P-rGO/CdSe QDs electrode was modified with 20 μL of the prepared afGQDs with the help of EDC (10 mg mL^{-1}) and NHS (10 mg mL^{-1}). The modified electrode was washed with ultrapure water to remove the physically adsorbed afGQDs. Finally, the "Z-scheme" PEC system based on P-rGO/CdSe QDs/afGQDs on the ITO electrode was obtained.

To immobilization of DNA1, GLD was used as cross-linking agent through the reaction between the amino group on the DNA1 and aldehyde group of the GLD. The ITO/P-rGO/CdSe QDs/afGQDs electrode was firstly soaked in 2.5% GLD solution for 1 h at room temperature, followed by rinsing with ultrapure water carefully to remove the adsorbed GLD. Then, the electrode was incubated with 1 μM DNA1 (10 mM Tris-HCl, 0.1 M NaCl , pH 7.4) for 12 h at 4 °C in darkness. After that, the electrode was washed thoroughly with 10 mM Tris-HCl (pH 7.4), followed by incubation with 20 μL of 1.0 % BSA for 1 h at 4 °C to avoid the nonspecific adsorption. After rinsed with 10 mM Tris-HCl (pH 7.4), the electrode was incubated

with 20 μL of the prepared DNA2-Au-PAMAM-Mn^{2+} bioconjugation for 2 h at 37 °C, and then washed with 10 mM Tris-HCl (pH 7.4). The formed double-strand DNA contained a specific recognition sequence (5'-CCGG-3') for both M.SssI MTase and HpaII.

The electrode was further incubated with 20 μL of the 1× NEBuffer 2 containing various concentrations of M.SssI MTase and 160 μM sadenosyl-L-methiolnine for 2 h at 37 °C to catalyze the methylation of the specific CpG dinucleotides. After that, the methylated electrode was washed with 10 mM Tris-HCl (pH 7.4). The digestion of unmethylated DNA by restriction endonuclease HpaII which recognized the 5'-CCGG-3' sequence was carried out by incubating the electrode with 20 μL of the 1×CutSmart buffer containing 40 U mL^{-1} HpaII for 2 h at 37 °C. After washed thoroughly with 10 mM Tris-HCl (pH 7.4), the electrode was treated the 10 mM $KMnO_4$ solution for 60 s at ambient temperature to form the DNA2-Au-PAMAM-MnO_2 bioconjugation on the electrode. Finally, the electrode was incubated with 5 mM 4-CN solution for 30 min and 4-CN was transferred to the insoluble 4-CD on the electrode. After the electrode was washed with 10 mM Tris-HCl (pH 7.4), PEC measurements of the obtained electrode were performed in 0.1 M PBS (pH 7.4) containing 0.1M AA at room temperature with a applied potential of -0.1 V.

7. Inhibition assay of M. SssI MTase.

The inhibition effects of 5-azacytidine (5-Aza) and 5-aza-2′-deoxycytidine (5-Aza-dC) on the activity of M.SssI MTase were investigated as follows: the ITO/P-

rGO/CdSe QDs/afGQDs/DNA1/BSA/DNA2-Au-PAMAM-Mn^{2+} electrode was incubated with 20 μL of the 1×NEBuffer 2 consisting of 60 U mL^{-1} M.SssI MTase, 160 μM SAM and different concentrations of inhibitors for 2 h at 37 °C. Then, the processes of HpaII digestion and the precipitation reaction of 4-CN, and PEC measurements were carried out according to the procedures shown in the M.SssI MTase activity assay.

8. Characterization of P-rGO, CdSe QDs, afGQDs and P-rGO/CdSe QDs/afGQDs

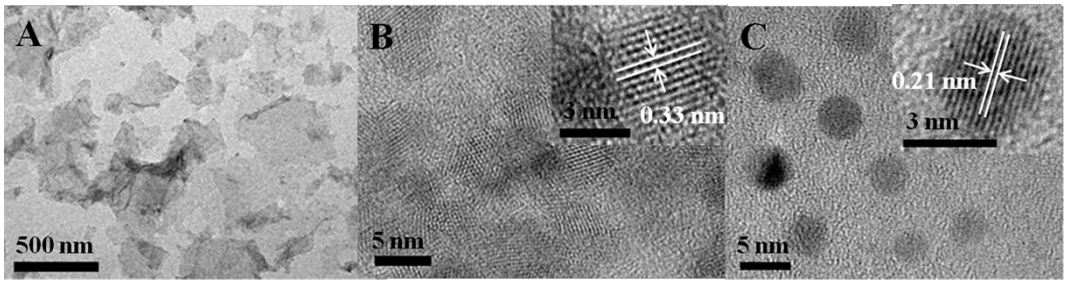

Fig. S1. TEM images of (A) P-rGO, (B) CdSe QDs and (C) afGQDs.

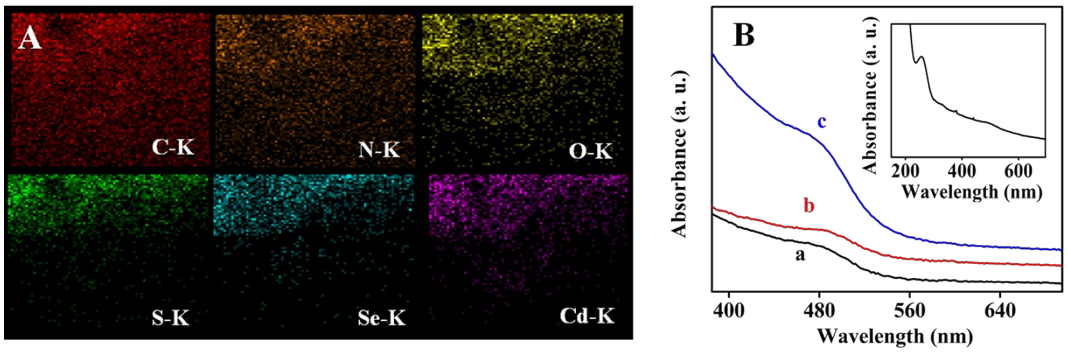

Fig. S2. (A) Elemental mapping images of the highlighted region in Fig. 1A. (B) UV-vis absorption spectra of (a) CdSe QDs, (b) P-rGO/CdSe QDs, and (c) P-rGO/CdSe QDs/afGQDs. The inset is the UV-vis absorption spectrum of afGQDs.

9. Characterization of the ITO/P-rGO/CdSe QDs/afGQDs electrode

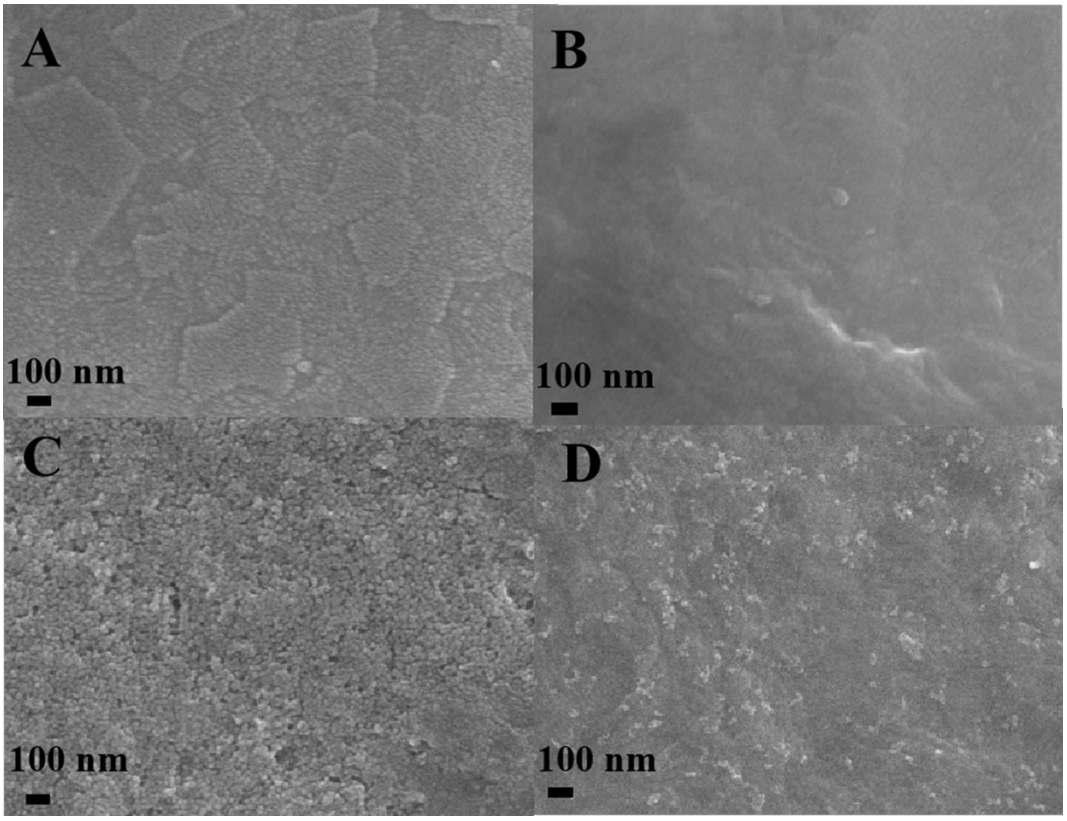

Fig. S3. SEM images of (A) bare ITO, (B) ITO/P-rGO, (C) ITO/P-rGO/CdSe QDs, (D) ITO/P-rGO/CdSe QDs/afGQDs electrodes.

The surface morphology of the bare ITO, ITO/P-rGO, ITO/P-rGO/CdSe QDs, ITO/P-rGO/CdSe QDs/afGQDs electrodes was characterized by SEM and the corresponding results are shown in Fig. S3. From Fig. S3A, it is noted that there are lots of indium-tin oxide particles on the ITO surface.[5] Compared with the ITO surface, the surface of ITO/P-rGO (Fig. S3B) becomes more smooth due to the sheet morphology of P-rGO. However, when the ITO/P-rGO electrode is modified with CdSe QDs, the surface of the ITO/P-rGO/CdSe QDs electrode becomes rough and lots of particles exist due to the aggregation of CdSe QDs (Fig. S3C). When the

ITO/P-rGO/CdSe QDs electrode is further modified with afGQDs, the electrode surface becomes more smooth again (Fig. S3D). These indicate that the ITO/P-rGO/CdSe QDs/afGQDs electrode is successfully prepared according to Scheme 1.

10. Cathodic and anodic linear potential scans

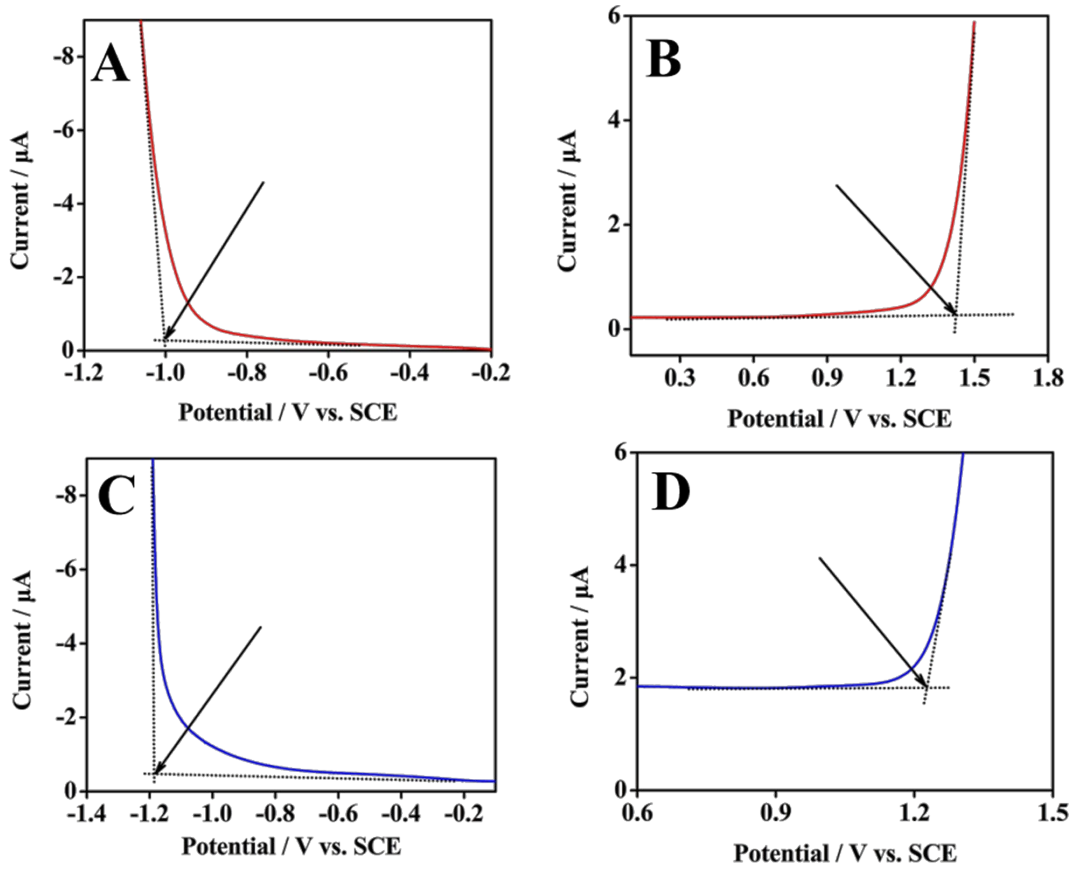

Fig. S4. Cathodic and anodic linear potential scans for determining the conduction band (CB) and valence band (VB) edges of CdSe QDs (A, B) and afGQDs (C, D) at 0.005 Vs^{-1} in N_2-saturated 0.1 M PBS (pH 7.4). (A) CdSe QDs with cathodic scan; (B) CdSe QDs with anodic scan; (C) afGQDs with cathodic scan; (D) afGQDs with anodic scan.

In order to clearly clarify the mechanism of the switching of photocurrent-polarity, the conduction band (CB) and the valence band (VB) of the CdSe QDs and afGQDs were investigated by cyclic voltammetry (CV) (Fig. S4).[6,7] The CB and VB edges of CdSe QDs can be observed at -1 V and 1.42 V, while the CB and VB edges of afGQDs can be observed at -1.19 V and 1.22 V vs. SCE. That is, the CB and VB

potentials of CdSe QDs are -0.76 and 1.66 V, and those of the afGQDs are -0.95 V and 1.46 V vs. the normal hydrogen electrode (NHE), respectively.

11. Characterization DNA2-Au-PAMAM-Mn^{2+}

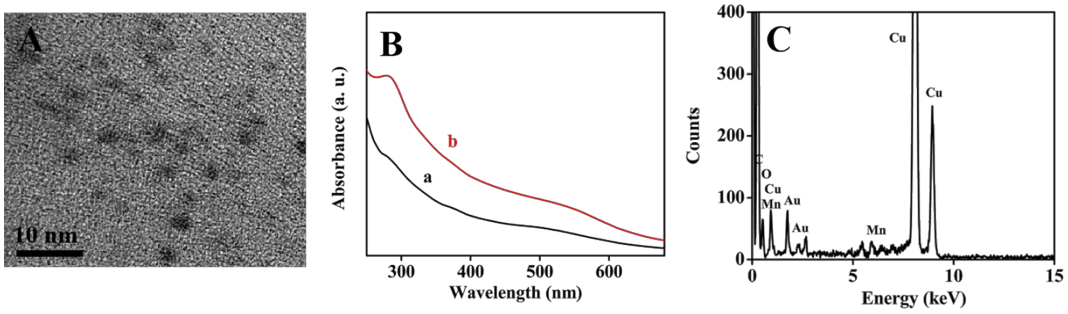

Fig. S5. (A) TEM of Au-PAMAM. (B) UV-vis absorption spectra of (a) Au-PAMAM and (b) DNA2-Au-PAMAM. (C) EDX spectrum of DNA2-Au-PAMAM-Mn^{2+}.

12. Characterization of MnO_2 on the electrode surface

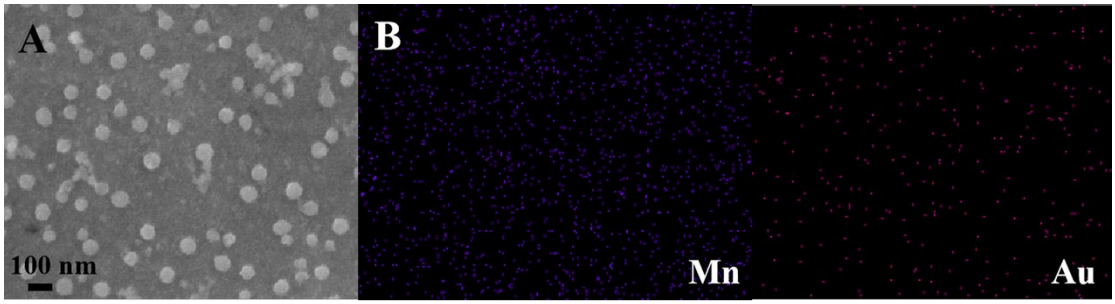

Fig. S6. (A) SEM image and (B) EDX mapping of the ITO/P-rGO/CdSe QDs/afGQDs/DNA1/BSA/ DNA2-Au-PAMAM-Mn^{2+} electrode treated with $KMnO_4$ solution.

After the ITO/P-rGO/CdSe QDs/afGQDs/DNA1/BSA/DNA2-Au-PAMAM-Mn^{2+} electrode was treated with $KMnO_4$ solution, the morphology of the electrode was investigated by SEM. From Fig. S6A, MnO_2 nanoparticles with an average diameter

of 70 nm are observed on the electrode surface. Further, from the EDX mapping results shown in Fig. S6B, it clearly displays the uniform distribution of Mn and Au on the modified electrode surface. The above results imply that the ITO/P-rGO/CdSe QDs/afGQDs/DNA1/BSA/DNA2-Au-PAMAM-MnO_2 electrode is obtained.

13. The photoluminescence spectrum of afGQDs and UV-vis absorption spectrum of Au-PAMAM

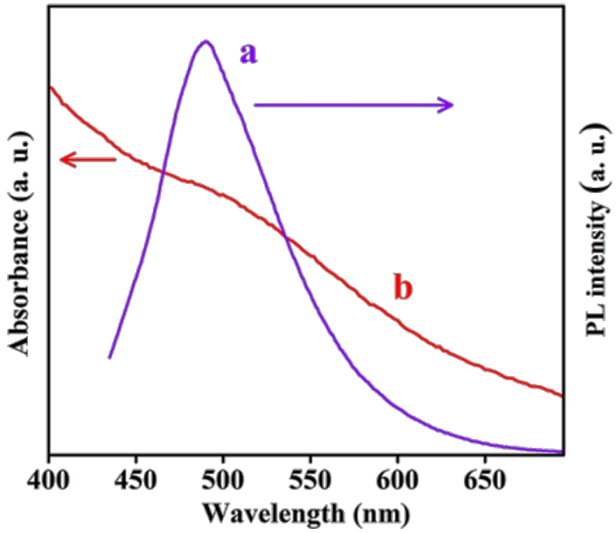

Fig. S7. Photoluminescence spectrum of afGQDs (a) and UV-vis absorption spectrum of Au-PAMAM (b).

As shown in Fig. S7, the emission band of afGQDs is observed at 492 nm while the absorption band of Au-PAMAM is located at around 520 nm. Obviously, the emissions of afGQDs have a considerable spectral overlap with the absorption of the Au-PAMAM, which is beneficial to trigger the energy transfer (ET) between afGQDs and Au NPs.[8]

14. The percentage of each inhibition effect

As shown in Fig. 2B, the photocurrent of the ITO/P-rGO/CdSe QDs/afGQDs/DNA1/BSA electrode (curve f) is -16.15 μA (I_f). After the introduction of DNA_2-Au-PAMAM-Mn^{2+} and incubation with M.SssI MTase and HpaII endonuclease successively (curve h), the photocurrent of the electrode decreases to -13.35 μA (I_h), owing to the energy transfer effect between afGQDs and Au NPs. When the modified electrode is further treated with $KMnO_4$ solution (curve i), the photocurrent of the electrode further decreases to -11.34 μA (I_i), due to the steric hindrance effect of Au-PAMAM-MnO_2. After the electrode was incubated with 4-CN solution, a sharp decrease of the photocurrent can be observed (curve j, I_j, -5.692 μA) because of the precipitation effect of 4-CD.

The total decrease of photocurrent signal inhibited by the energy transfer effect between afGQDs and Au NPs, the steric hindrance effect of Au-PAMAM-MnO_2, and the precipitation effect of 4-CD is 10.458 μA ($\Delta I = I_j - I_f$). The percentage of photocurrent signal inhibited by the energy transfer effect between afGQDs and Au NPs is about 27% ($[(I_h - I_f)/\Delta I]\times 100\%$), while the percentage of photocurrent signal inhibited by the steric hindrance effect of Au-PAMAM-MnO_2 is about 19% ($[(I_i - I_h)/\Delta I]\times 100\%$). In addition, the percentage of photocurrent signal inhibited by the precipitation effect of 4-CD is about 54% ($[(I_j - I_i)/\Delta I]\times 100\%$). These results indicate that the inhibition efficiency of the precipitation effect of 4-CD is larger than that of the energy transfer effect between afGQDs and Au NPs, and the steric hindrance effect of Au-PAMAM-MnO_2.

15. Optimization of experimental conditions.

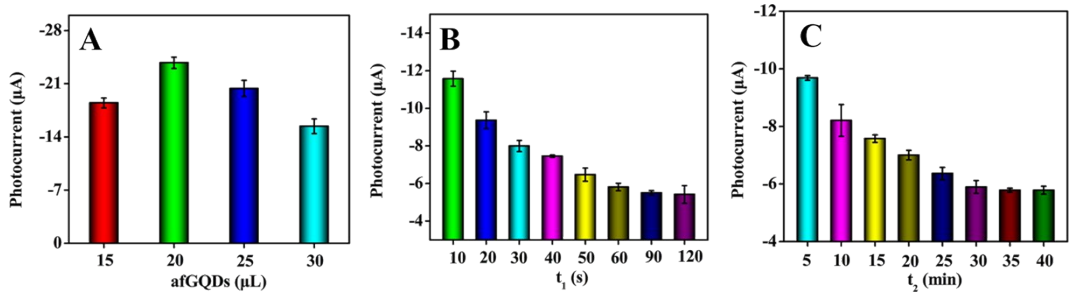

Fig. S8. (A) Influence of the added volume of afGQDs on the photocurrent of the ITO/P-rGO/CdSe QDs/afGQDs electrode in 0.1 M PBS (pH 7.4) containing 0.1 M AA at -0.1 V. (B) Influence of the incubation time (t_1) of $KMnO_4$ solution (afGQDs, 20 μL; M.SssI MTase, 50 U ml^{-1}; incubation time (t_2) of 4-CN solution, 30 min) and (C) incubation time (t_2) of 4-CN solution (afGQDs, 20 μL; M.SssI MTase, 50 U ml^{-1}; incubation time (t_1) of $KMnO_4$ solution, 60 s) on the photocurrent of the proposed PEC biosensor.

In order to obtain the excellent analytical performance of the developed PEC biosensor, the following parameters, such as the added volume of afGQDs, the incubation time (t_1) of $KMnO_4$ solution and incubation time (t_2) of 4-CN solution, were investigated (Fig. S8).

The added volume of afGQDs plays a vital role on the photocurrent of the ITO/P-rGO/CdSe QDs/afGQDs electrode. Fig. S8A shows that the photocurrent of the ITO/P-rGO/CdSe QDs/afGQDs electrode increases with the increase of the afGQDs added volume and a maximum is obtained at 20 μL. So, 20 μL is selected as the optimal volume of afGQDs.

The incubation time (t_1) of the ITO/P-rGO/CdSe QDs/afGQDs/DNA1/BSA/ DNA2-Au-PAMAM-Mn^{2+} electrode in $KMnO_4$ solution is one of the key parameters for the analytical performance of the biosensor. As shown in Fig. S8B, the photocurrent of the PEC biosensor decreases with the increasing t_1, and reaches a plateau at 60 s. Therefore, 60 s is used as the optimum t_1.

After the ITO/P-rGO/CdSe QDs/afGQDs/DNA1/BSA/DNA2-Au-PAMAM-Mn^{2+} electrode was treated with M.SssI MTase/HpaII and $KMnO_4$ solutions, the electrode was incubated with 4-CN solution. The incubation time (t_2) was also investigated and the results are shown in Fig. S8C. When the t_2 increases, the photocurrent of the biosensor decreases and a plateau can be obtained at about 30 min. Hence, 30 min is selected as the optimum t_2.

16. Influences of Inhibitors on M.SssI MTase activity

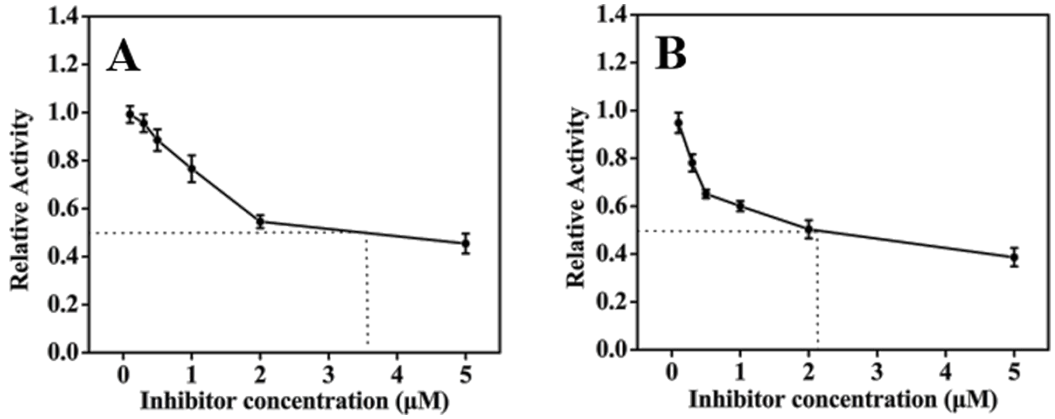

Fig. S9. The influences of the inhibitors 5-Aza (A) and 5-Aza-dC (B) on the M.SssI MTase activity.

In order to further study the potential application of the proposed biosensor in screening the inhibitor, 5-azacytidine (5-Aza) and 5-aza-2′-deoxycytidine (5-Aza-dC)

were employed as the model inhibitors. These compounds, which can inactivate DNA MTase, are nucleoside analogues and representative anticancer drugs used in the majority of methylation inhibition experiments and a large number of clinical trials. The relative activity (%) is calculated as follows: relative activity = $(I_0-I_i)/(I_0-I_t) \times 100\%$. Where I_0, I_t, and I_i represent the photocurrent in the absence of M.SssI MTase, in the presence of M.SssI MTase, and in the presence of both M.SssI MTase and inhibitor, respectively. As observed in Fig. S9, with the increase of inhibitor concentration, the relative activity of M.SssI MTase decreases gradually. The results reveal that the activity of M.SssI MTase is inhibited and the methylated DNA on electrode surface is reduced, leading to a decreased immobilization amount of double-strand DNA and further an increase in photocurrent signal. The inhibiting efficiency of the inhibitors can be expressed as the IC_{50} value, which represents the inhibitor concentration demand for 50 % decrease in enzyme activity. From Fig. S11, the IC_{50} values for 5-Aza and 5-Aza-dC can be obtained about 3.6 μM and 2.1 μM, respectively. These results demonstrate that the prepared PEC biosensor can be utilized to screen the inhibitors of DNA MTase.

17. Stability, reproducibility and selectivity of the PEC biosensor

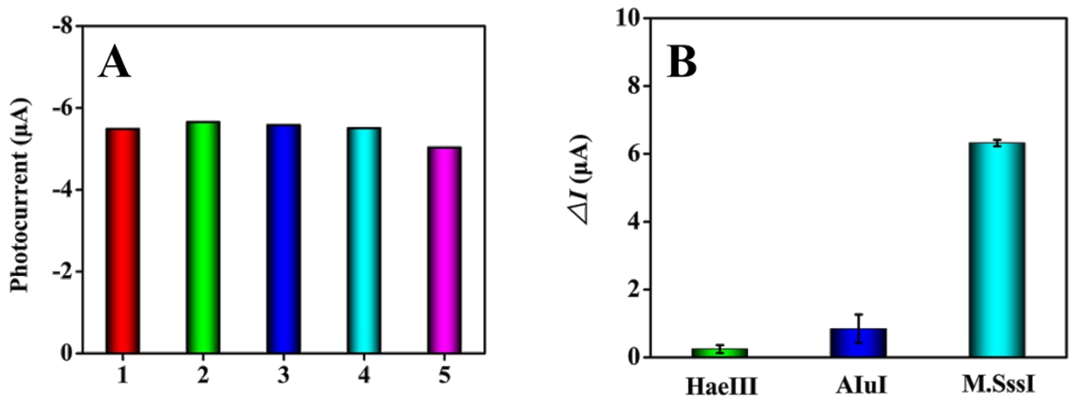

Fig. S10. (A) Reproducibility of the PEC biosensor incubated with 50 U mL^{-1} M.SssI MTase in the same batch. (B) Selectivity of the PEC biosensor towards M.SssI MTase. AluI, 100 U mL^{-1}; HaeIII, 100 U mL^{-1}; M.SssI, 50 U mL^{-1}.

The stability of the developed PEC biosensor was also investigated by storing the ITO/P-rGO/CdSe QDs/afGQDs/DNA1/BSA electrode at 4 °C in the refrigerator for 2 weeks. The photocurrent response can retain about 94.9% of the initial value for 50 U mL^{-1} M.SssI MTase. The reproducibility of the proposed PEC biosensor is also investigated. As shown in Fig. S10A, the relative standard deviation (RSD) for five modified electrodes is 4.5%. These results suggest that the proposed PEC biosensor has the satisfactory stability and reproducibility for M.SssI MTase activity assay.

To investigate the selectivity, HaeIII and AluI MTase were chosen as the potential interfering enzymes and the results are shown in Fig. S10B. The photocurrent responses ΔI ($\Delta I = I - I_0$, I_0 and I stand for the photocurrent values of the developed PEC biosensor in blank solution and in the solution with M.SssI MTase or interferents, respectively) towards M.SssI MTase is much larger than that towards HaeIII or AluI MTase, which clearly suggests that the prepared PEC biosensor possesses acceptable selectivity.

18. Comparison of various methods for M.SssI MTase activity assay

Table S2. Comparison of various methods for M.SssI MTase activity assay.

Method	Linear range ($U\ mL^{-1}$)	Detection limit ($U\ mL^{-1}$)	Reference
Electrochemistry	0.5-50	0.1	9
Electrochemistry	0.1-450	0.05	10
Electrochemistry	0.5-60	0.09	11
Electrochemistry	0.5-355	0.1	12
Surface-enhanced Raman spectroscopy	0.1-10	0.067	13
Electrochemiluminescence	0.05-100	0.02	14
Circular dichroism spectroscopy	0.5-150	0.27	15
Photoelectrochemical	1-50	0.33	16
Photoelectrochemical	1-80	0.316	17
Photoelectrochemical	5-80	0.45	18

Photoelectrochemical	0.1-60	0.046	This work

19. References

1 L. L. Li, K. P. Liu, G. H. Yang, C. M. Wang, J. R. Zhang and J. J. Zhu, *Adv. Funct. Mater.,* 2011, **21,** 869–878.

2 Z. L. Qiu, J. Shu and D. P. Tang, *Anal. Chem.,* 2017, **89,** 5152−5160.

3 J. Peng, W. Gao, B. K. Gupta, Z. Liu, R. Romero-Aburto, L. H. Ge, L. Song, L. B. Alemany, X. B. Zhan, G. H. Gao, S. A. Vithayathil, B. A. Kaipparettu, A. A. Marti, T. Hayashi, J. J. Zhu and P. M. Ajayan, *Nano Lett.* 2012, **12,** 844–849.

4 J. Han, Y. Zhuo, Y. Q. Chai, G. F. Gui, M. Zhao, Q. Zhu and R. Yuan, *Biosens. Bioelectron.* 2013, **50,** 161–166.

5 G. C. Fan, H. Zhu, D. Du, J. R. Zhang, J. J. Zhu and Y. Lin, *Anal. Chem.* 2016, **88,** 3392–3399.

6 G. L. Wang, J. X. Shu, Y. M. Dong, X. M. Wu, W. W. Zhao, J. J. Xu and H. Y. Chen, *Anal. Chem.,* 2015, 87, 2892–2900.

7 L. Y. Jin, Y. M. Dong, X. M. Wu, G. X. Cao and G. L. Wang, *Anal. Chem.,* 2015, 87, 10429–10436.

8 M. Zhao, G. C. Fan, J. J. Chen, J. J. Shi and J. J. Zhu, *Anal. Chem.* 2015, **87,** 12340–12347.

9 M. Wang, Z. N. Xu, L. J. Chen, H. S. Yin and S. Y. Ai, Anal. Chem. 2012, 84, 9072–9078.

10 W. Li, P. Wu, H. Zhang and C. X. Cai, *Anal. Chem.* 2012, **84,** 7583–7590.

11 J. J. Ji, Y. J. Liu, W. Wei, Y. J. Zhang and S. Q. Liu, *Biosens. Bioelectron.* 2016, **85,** 25–31.

12 S. N. Liu, P. Wu, W. Li, H. Zhang and C. X. Cai, *Chem. Commun.* 2011, **47,** 2844–2846.

13 P. P. Hu, H. Liu, S. J. Zhen, C. M. Li and C. Z. Huang, *Biosens. Bioelectron.* 2015, **73,** 228–233.

14 Y. Li, C. C. Huang, J. B. Zheng and H. L. Qi, *Biosens. Bioelectron.* 2012, **38,** 407–410.

15 Y. J. Liu, M. Wei, L. Q. Zhang, W. Wei, Y. J. Zhang and S. Q. Liu, *Chem. Commun.* 2015, **51,** 14350–14353.

16 Z. Q. Yang, F. R. Wang, M. Wang, H. S. Yin and S. Y. Ai, *Biosens. Bioelectron.*. 2015, **66,** 109–114.

17 H. Y. Wang, P. Liu, W. J. Jiang, X. Li, H. S. Yin and S. Y. Ai, *Sens. Actuators, B.* 2017, **244,** 458–465.

18 X. Liu, C. H. Wei, J. Luo, Y. P. Wu, X. Y. Guo, Y. Ying, Y. Wen and H. F. Yang, *Microchim. Acta* 2018, **185,** 498–504.